

# An Optically Readable InGaN/GaN RRAM

K. Zheng, J. L. Zhao, Z. H. Zhang, Y. Ji, B. B. Zhu, S. T. Tan, H. V. Demir, K. L. Teo, and X. W. Sun

**Abstract**—The unidirectional bipolar resistance switching in GaN/InGaN-based light-emitting diode (LED) was discovered to explore optically readable resistive random access memory (RRAM) device. The device displays stable resistance window in both endurance and retention tests, showing good nonvolatility for memory application. The light-emitting state of this device can also be tuned by the resistance switching. Such phenomenon is illustrated as the switching between conventional light-emitting rectifying behavior and nonlight-emitting metal-like ohmic behavior. Large amount of structural and point defects in the epitaxial wafer were considered as the main contributor to the resistance switching in LED device.

**Index Terms**—Defect, filament, GaN, light-emitting diode (LED), resistive random access memory (RRAM).

## I. INTRODUCTION

AS ONE of the most promising candidates for the next generation memory, resistive random access memory (RRAM) has achieved remarkable development in the last two decades. By virtue of its simplicity both in device configuration and operation principle, some pioneering work has been done to explore the multifunctional devices by combining the resistance switching (RS) property with other optoelectronic devices [1], [2], such as the memristor with tunable electroluminescence (EL) [3] and the light-controlled multilevel switching RRAM [4]. As well accepted by the community, filament formation associated with defects is the origin of the most RS phenomenon. The completeness of the conductive filament throughout certain bulk material defines the two different resistance states, while the migratable defects in the RS material directly contribute to the filament dynamic. Defect is also a challenging topic in the InGaN/GaN multiple quantum well (MQW) light-emitting diode (LED).

Manuscript received May 14, 2015; revised April 1, 2016; accepted April 1, 2016. Date of publication April 21, 2016; date of current version May 19, 2016. This work was supported by the National Research Foundation, Singapore, through the Competitive Research Programme administered by Nanyang Technological University under Grant NRF-CRP11-2012-01 and Grant NRF-CRP6-2010-2. The review of this paper was arranged by Editor S. Bandyopadhyay.

K. Zheng, Z. H. Zhang, Y. Ji, B. B. Zhu, S. T. Tan, and H. V. Demir are with the School of Electrical and Electronic Engineering, Nanyang Technological University, Singapore 639798 (e-mail: zhengke@ntu.edu.sg; zh.zhang@ntu.edu.sg; jiyu0004@e.ntu.edu.sg; zhuh0002@e.ntu.edu.sg; sweetiam@ntu.edu.sg; hvdemir@ntu.edu.sg).

J. L. Zhao and K. L. Teo are with the Department of Electrical and Computer Engineering, National University of Singapore, Singapore 117608 (e-mail: jlzhao@hotmail.sg; eleteokl@nus.edu.sg).

X. W. Sun is with the School of Electrical and Electronic Engineering, Nanyang Technological University, Singapore 639798, and also with the Department of Electrical and Electronic Engineering, College of Engineering, South University of Science and Technology, Shenzhen 518055, China (e-mail: exwsun@ntu.edu.sg).

Color versions of one or more of the figures in this paper are available online at <http://ieeexplore.ieee.org>.

Digital Object Identifier 10.1109/TED.2016.2550506

Both structural defect (i.e. threading dislocation/V defect) and point defects (i.e., nitrogen vacancies, Mg–H complex) in such LED devices account for the nonradiative recombination and leakage current during operation, which leads to the efficiency droop at higher injected current [5], [6]. These defects are troublesome in LED but sometimes favorable for RRAM, because the operation of the RRAM is defect related. The apparent contradiction could be converted into excellent combination of these two functional devices as long as the defects are well manipulated. Our previous work has already discovered that the p-n junction could produce unidirectional bipolar RS between rectifying and ohmic behavior [7]. The reverse bias softly breaks down the junction into ohmic characteristic in the SET process, and the forward bias recovers the junction to rectifying behavior in the RESET process. In this paper, similar properties were also found in the defective InGaN/GaN LED. The coexistence of resistance switching and light emitting in such device was analyzed in detail. The switching between two different resistance states directly tuned the light-emitting behavior. Therefore, a bifunctional device, the so-called optically readable RRAM or in-LED memory, was successfully realized. Such device will either improve the serial electrical reading process of RRAM with the assistance of parallel optical reading [4] or enrich each single LED cell with data storage ability. Therefore, our result offers an alternative way in developing the next generation of optoelectronic devices.

## II. EXPERIMENTAL DETAIL

InGaN/GaN LED wafers in this paper were grown by a metal–organic chemical vapor deposition (MOCVD) system and patterned by photolithography on the 2-in c-sapphire substrate. The growth started with a 30-nm lightly Si-doped GaN (u-GaN) buffer, followed by a 4- $\mu\text{m}$  u-GaN as a template for subsequent epitaxial growth. A 2- $\mu\text{m}$  Si-doped n-GaN was grown right before the deposition of eight-period of InGaN/GaN QWs. AlGaIn with a thickness of 20 nm was deposited as an electron blocking layer, and finally, the structure was covered by a 200 nm of Mg-doped p-GaN [8], [9]. The indium contact with a diameter of 1  $\mu\text{m}$  was made on the wafer for electric and optic characterization. An integrating sphere with the Ocean Optics spectrometer was employed to measure the EL of LED. The  $I$ – $V$  and capacitance–voltage ( $C$ – $V$ ) characterizations were carried out on a probe station with the Keithley 4200 SCS semiconductor parameter analyzer.

## III. RESULT AND DISCUSSION

In common LED devices, the light emitting usually takes place in forward bias, while only a small leakage current

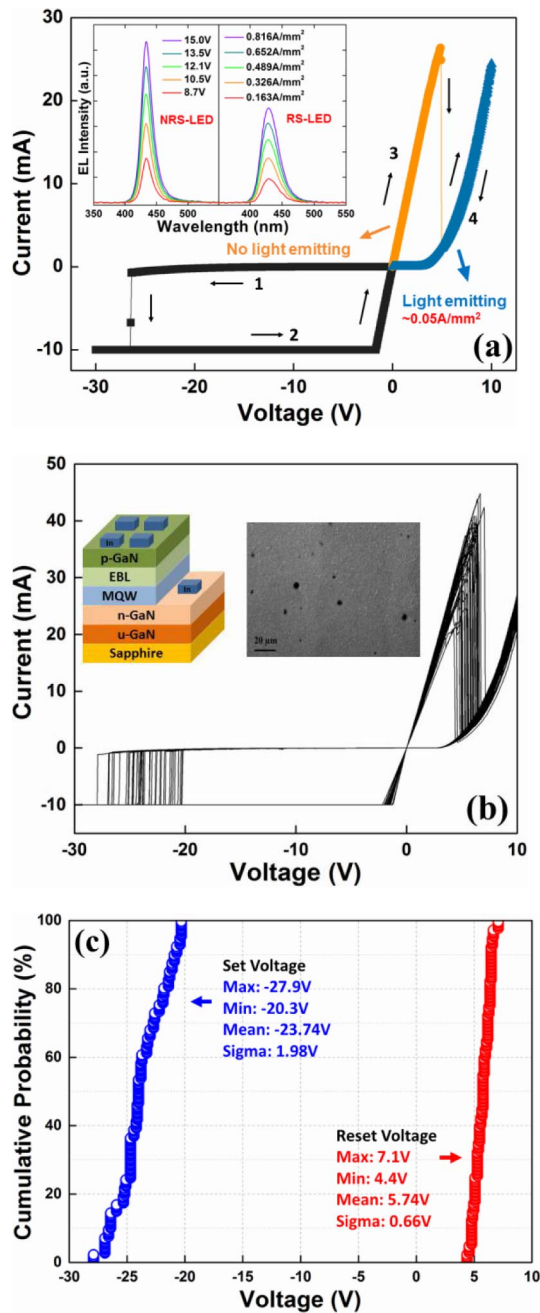


Fig. 1. (a) Resistive switching of as-prepared LED wafer. Inset: EL spectra comparison between NRS-LED and RS-LED. (b) Multiple RS cycles drawn in linear scale. Inset: device schematic and SEM image of defective wafer surface. (c) Cumulative probability plotting of SET and RESET voltages.

could be detected with negative bias, which is also described as rectifying behavior. A permanent breakdown (or hard breakdown) will occur when the negative voltage is high enough. However, beyond this normal LED behavior, an RS phenomenon was observed in our device with specific operation. A typical RS cycle of InGaN/GaN LED is shown in Fig. 1(a). If a compliance current of 10 mA is applied during the negative sweep, the breakdown triggered at the region of over  $-20$  V is soft, which could be recovered by the next positive sweep. Such process is defined as SET, and the device switches from the high resistance state (HRS) to the low resistance state (LRS) as indicated by a sudden current increase.

When the subsequent positive bias is applied, the device still maintains LRS with high current in the low-voltage region, corresponding to the nonvolatile data storage. However, the device shows no light emitting in this region [Fig. 1(a) (orange region)]. When the forward sweep proceeds to another threshold value (usually over 4 V), the current abruptly drops down with the appearance of a visible blue light emitting at the current density of  $\sim 0.05$  A/mm<sup>2</sup> [Fig. 1(a) (blue region)]. Such process is defined as RESET and the device is switched to HRS again. The turn-ON voltage for defective LED device is usually  $\sim 4$  V. Therefore, the light emitting could be clearly detected after the RESET threshold point. As the positive sweep continues, a gradual increase in both current and light-emitting intensity is observed, which confirms the restoration of light-emitting capability and the rectifying behavior of LED.

To summarize, a bistable bipolar RS is obtained between the nonlight-emitting LRS and the light-emitting HRS. Such RS phenomenon cannot be observed in high-quality InGaN/GaN LED, but only the defective ones. Fig. 1(a) (inset) shows the EL spectra comparison between the nonresistive-switching LED (NRS-LED) and the resistive-switching LED (RS-LED). With different injection current densities from 0.163 to 0.816 A/mm<sup>2</sup>, the light-emitting intensity of a defective LED (at HRS status) is apparently lower than a common high-quality one. In other words, a tradeoff has to be made between the RS ability and the light-emitting efficiency. Multiple switching cycles were shown in Fig. 1(b) with the inset showing the device schematics and the SEM image of the wafer surface. Fig. 1(c) shows the cumulative probability plotting of SET and RESET voltages. The SET window ( $-20.3$  to  $-27.9$  V) is a bit larger than the RESET window ( $4.4\sim 7.1$  V) as indicated in the data summary. Despite such fluctuation of operation voltages, the device still shows stable repeating cycles. Reading voltage is fixed at 1 V for safely reading out the corresponding storage status. It obviously does not overlap with the SET window and will not affect each present resistive status.

The resistance distribution in 200 repeating cycles is shown in Fig. 2(a), with a stable resistance window of about three orders. The retention test was also taken at room temperature and 85 °C, as shown in Fig. 2(b). Both resistances in HRS and LRS display little decay over  $10^5$  s, showing good nonvolatility for RRAM applications. As the temperature increases, the LRS resistance increases slightly according to the property of metallic filament, while the HRS resistance declines which corresponds to the transport characteristics of semiconductor.

As we mentioned earlier, high-epitaxial-quality InGaN/GaN LED wafer could not produce RS behavior. However, such RS phenomenon is prominent in some defective wafers. The defect-related issues in GaN-based LED have been studied intensively, because it has been one of the most serious obstacles for high-power solid-state lighting. The lowering of internal quantum efficiency in high current injection is attributed to the inevitable threading dislocation (density usually around  $10^8$  cm<sup>-2</sup>) and other point defects in the thin film stacks. The V defects associated with threading dislocation on the surface of our LED wafer were examined, as shown in the SEM image in Fig. 1(b). These defects introduce the deep level

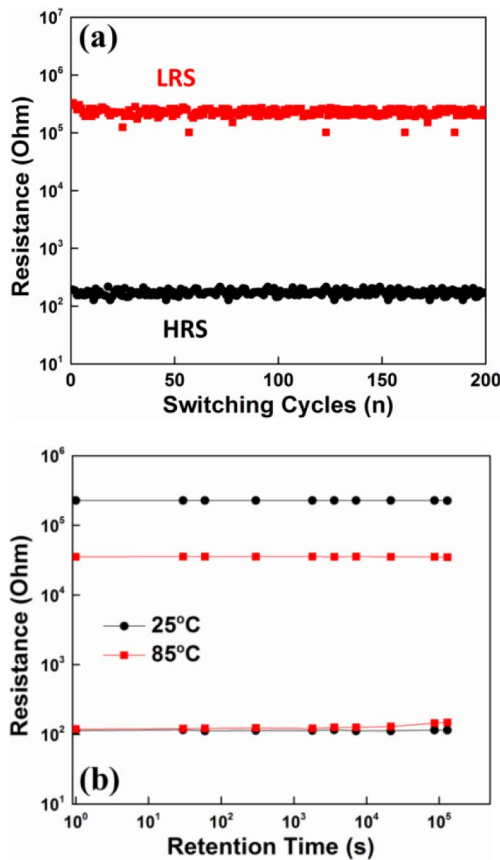


Fig. 2. (a) RS endurance performance of defective LED. (b) RS retention performance at 25 °C and 85 °C.

traps, which assist the carrier tunneling and leakage current under both forward and reverse biases [10]. Such defect-related carrier transport plays an even more important role in the SET process (reverse bias). Here, the forward and reverse  $I$ - $V$  curves of light-emitting HRS are plotted in the semilog scale at different temperatures, as shown in Fig. 3.

The forward  $I$ - $V$  characteristics in Fig. 3(a) can be represented as  $I = I_0 \exp(qV/E)$ , where  $I_0$  is a preexponential factor and  $E$  is an energy parameter. At room temperature, the calculated  $E$  at the voltage region of 2.3~3.2 V is 208 meV. Assuming  $E = nkT$ , an unrealistic ideality factor  $n$  of 8.1 can be extracted. Usually,  $n = 1$  indicates the domination of diffusion current, while  $n = 2$  indicates the domination of recombination current. The much larger ideality factor obtained here stands for a typical tunneling current in the space-charge region [11]. Moreover, the slope shows little dependence of temperature, which is another feature of carrier tunneling [12]. Therefore, the forward current in the defective LED consists of diffusion, recombination, and tunneling components. The tunneling process mainly takes place at the interfaces of MQW/cladding layers and within MQW region, with nonradiative recombination at deep level traps, including nitrogen vacancies, oxygen impurities Mg-H complex, and threading dislocation in the thin-film stacks [11], [13].

The reverse current in Fig. 3(b) is of much larger magnitude than the conventional diffusion and recombination current, which also indicates the existence of carrier tunneling. The current is not only field-dependent but also

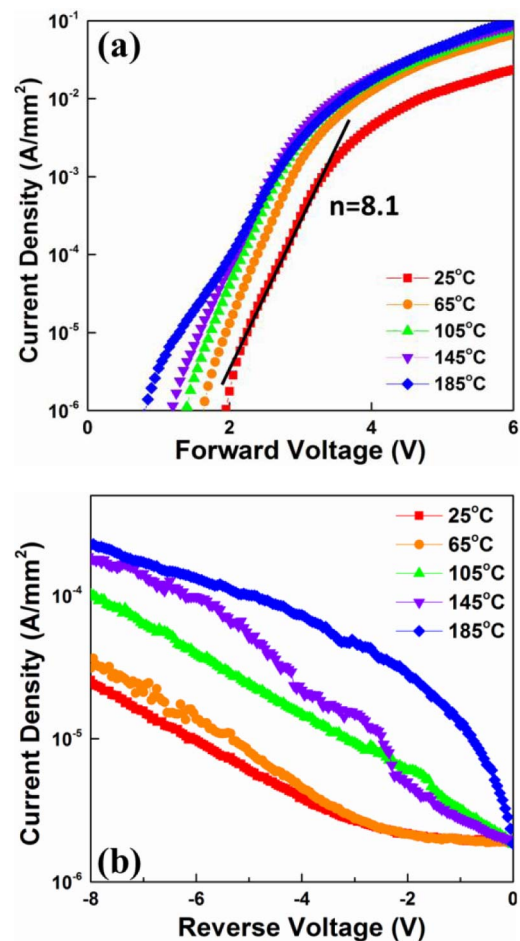


Fig. 3. (a) Forward and (b) reverse  $I$ - $V$  curves of light-emitting state at different temperatures drawn in log ( $I$ )- $V$  scale.

temperature-dependent in the lower voltage region, where the current increases much faster at higher temperature. Thus, a thermal-assisted generation process is involved in the reverse leakage current here [14]. In the higher voltage region, the current shows lower temperature sensitivity, which indicates that the tunneling process gradually dominates the carrier transport [15]. In general, the low-field reverse tunneling is mainly due to defect-related traps, while in the high field, the band-to-band tunneling, such as Zener tunneling, becomes the major contributor. When the reverse bias is high enough, the soft breakdown will occur.

As is well known, the defects, especially the deep-level traps, will significantly affect the  $C$ - $V$  characteristics of p-n junctions. Therefore, the  $C$ - $V$  measurement of light-emitting HRS was also carried out in the dc sweep mode superimposed by a 30-mA ac voltage at the frequencies of 10 kHz and 1 MHz. As shown in Fig. 4, the parallel capacitance increases and arrives at the peak value at around 4 V in the low positive field region due to the narrowing of space-charge region with applied voltage. However, with the further increase in the voltage, the positive capacitance starts to decrease and even enters the negative region, which is called negative capacitance (NC) phenomenon. Moreover, light emission is observed, as the capacitance begins to decrease and the intensity increases as the NC becomes stronger. As been

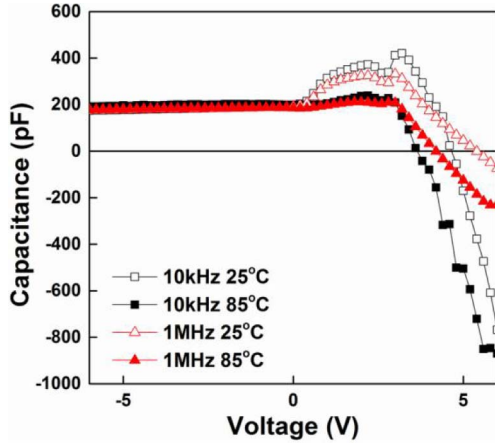


Fig. 4.  $C$ - $V$  curves with different ac frequency and temperature setups.

discussed previously, such NC relates to both nonradiative recombination of injected carriers in the deep traps and radiative recombination in the active region of LED [16]. When the forward bias reaches certain value, the recombination exceeds the diffusion and leads to the negative variation of carrier accumulation in the active region as the positive voltage increases. From the comparison, we can also see that the capacitance initially increases less but subsequently decreases much faster at lower frequencies and higher temperature, which coincides with the previous studies as well [17], [18].

To further investigate the RS mechanism, the conduction properties in both LRS and HRS are discussed in the following section. First, a typical SET cycle in the reverse bias is singled out and plotted in the log-log scale, as shown in Fig. 5(a). In LRS, the high current level with the slope of  $\sim 1.0$  confirms the existence of conductive filament [19] in the defective stacks and the ohmic conduction throughout the whole LED device. However, the conduction in HRS is much more complex. As we mentioned earlier, the high density of defect-related traps accounts for the large reverse leakage current. When the injected current density is extremely low in the voltage region of  $<0.5$  V, the current gain is super low due to the multibarrier blocking effect. As the voltage increases, the thermally generated carriers over injected carriers dominate the conduction which obeys Ohm's law (slope  $\sim 1.0$ ). Continuing injected carriers with increasing voltage will gradually fill the defect-related traps and cause a trap-to-trap tunneling or the so-called Mott hopping behavior, which contributes to the conduction [20]. With the bias sweeping until over 3.5 V, the slope increases to 3.32, indicating the change of conduction mechanism. A group of curves in this region at different temperatures are replotted in  $\text{Ln}(I/V) - V^{1/2}$  scale in Fig. 5(a) (inset). The excellent linear fitting of the curves is the evidence of Poole-Frenkel (PF) emission. The PF emission refers to the field-assisted thermal excitation of the carriers from the traps located in the bulk material into the conduction band, which could be depicted in the following model [21]:

$$J_{\text{PF}} \propto E \exp\left(\frac{-q(\varphi_B - \sqrt{qE}/\pi\epsilon_i)}{kT}\right) \quad (1)$$

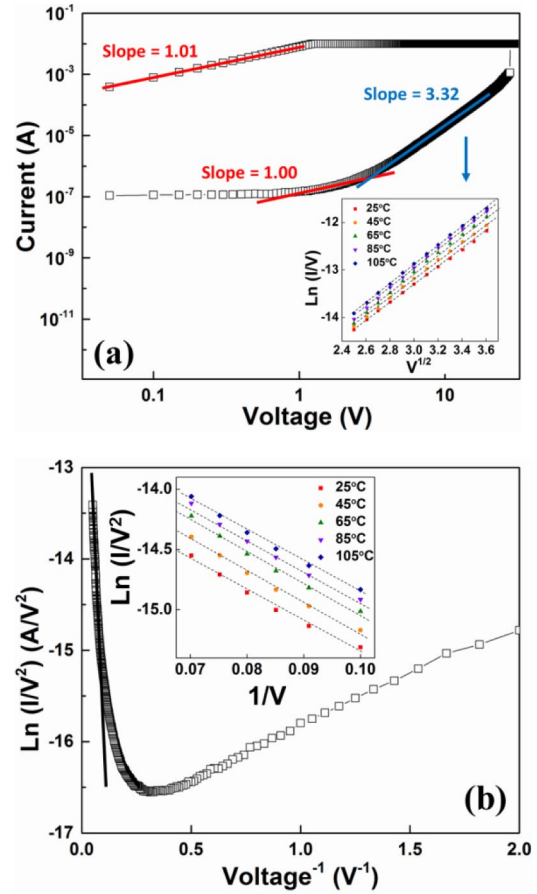


Fig. 5. (a)  $I$ - $V$  curve of the SET process plotted in log-log scale. Inset: linear fitting of PF emission at different temperatures. (b) HRS  $I$ - $V$  curve in  $\text{Ln}(I/V^2) - 1/V$  scale. Inset: linear fitting of FN tunneling at high-field region.

where  $J_{\text{PF}}$  is the current density,  $E$  is the electric field,  $\epsilon_i$  is the insulator permittivity,  $\varphi_B$  is the Coulombic barrier height raised by the interaction between positive traps and negative carriers,  $k$  is Boltzmann's constant, and  $T$  is the temperature. Here, the Schottky emission is ruled out, because the current in the high-voltage region shows very weak temperature dependence [both in Figs. 3(b) and 5(a) (inset)]. Actually, the PF emission here plays a significant role in trap-assisted tunneling. After the traps have all been filled, the intertrap hopping will not satisfy the conduction with further enhancement of the field. High field will effectively reduce the Coulombic barrier between the traps and the carriers, so the excess injection will force the captured carriers being detrapped from these defect sites into the conduction band and contribute to the current.

In general, the reverse conduction in such MQW LED with high density of defects is a really complicated combination of several mechanisms. When the voltage is high enough approaching the breakdown threshold, the barrier becomes sharpened especially in the MQW region. Thus, the electrons are able to traverse the barrier by Fowler-Nordheim (FN) tunneling and contribute to conduction, as shown in Fig. 6. The FN tunneling can be modeled as [22]

$$J_{\text{FN}} = K_1 E^2 \exp(-K_2/E) \quad (2)$$

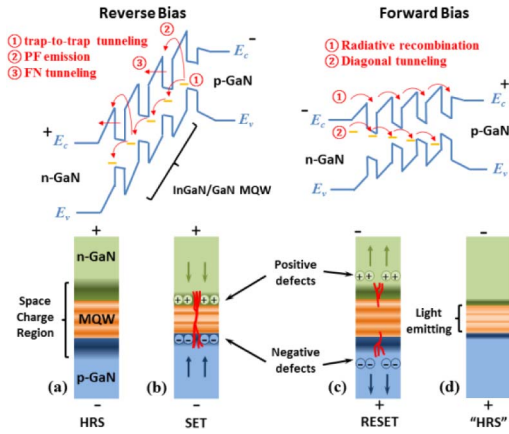


Fig. 6. Schematic of RS in defective GaN–InGaN LED. (a) HRS in reverse bias before SET. (b) Filament formation in reverse bias switches the device from HRS to LRS and no light emitting in small forward bias. (c) Filament rupture in forward bias switches the device from LRS to HRS again. (d) Light emitting restores in forward bias.

where

$$K_1 = \frac{q^3 m_e}{8\pi h m \phi_B} \quad (3)$$

and

$$K_2 = \frac{8\pi \sqrt{2m\phi_B^3}}{3qh} \quad (4)$$

where  $m_e$  is the electron mass in free space,  $m$  is the electron tunneling effective mass,  $\phi_B$  is the contact barrier height, and  $h$  is Planck's constant. As shown in Fig. 5(b), the HRS  $I$ – $V$  curve in reverse bias is plotted in  $\ln(I/V^2) - 1/V$  scale. At extra high-field region, the linear fitting can be obtained with temperature-independence [Fig. 5(b) (inset)]. Therefore, the FN tunneling is proved to exist in the defective LED as well. It should be noticed that the range of the above conduction processes may overlap, but do appear in order as ohmic conduction—PF emission—FN tunneling as the reverse bias increases. Beside the three main mechanisms, there may also be some other subordinate processes contributing to the reverse conduction, such as Schottky emission and direct tunneling at the interface barrier, or phonon-assisted tunneling via neutral defects [23]. However, the trap-assisted tunneling plays the dominant role in reverse conduction.

Although all the analyses above support the defect-related leakage current in the LED device, one critical point has not been taken into consideration yet. The RS in the LED is bipolar and unidirectional, which indicates that the transition between leakage path in HRS and conductive filament in LRS is dependent on the direction of the external field. Therefore, it is necessary to distinguish the mobile and immobile defects in LED which act differently in filament-based RS. The screw and mixed dislocations associate with V defects in MQW and cladding layers are immobile, but act like shunt resistors connecting the both sides of p–n junction [12]. The mobile point defects, such as nitrogen interstitial ( $N_i$ ) and nitrogen vacancies ( $N_v$ ), will migrate along the electric field.

Under large reverse bias, there will be an accumulation of positive  $N_v$  at the n side interface to form a highly n-doped region. As the same, another p-doped region by the accumulation of negative  $N_i$  at the p side interface will also form. Such activity will narrow the width of the depletion region and introduce higher density of defects, enabling the filament forming and penetrating throughout the whole active region [24]. Moreover, the injected carriers gained enough energy under the high electric field will also cause impact ionization and create more deep-level defects near the MQW/cladding layer interface, which also facilitates the formation of filament [14]. With the illustration in Fig. 6, the RS accompanied with tuned light emitting could be understood as follows.

- 1) In reverse bias, the deep-level traps assist the tunneling behavior, including intertrap hopping and PF emission. When the reverse field is high enough, the leakage current is further strengthened by FN tunneling. Meanwhile, the migration of defects toward the junction area narrows the space-charge region, and high density of defects finally link up as conductive filaments, which breakdown the whole active region to LRS (SET). The tunneling leakage is replaced by metal-like conduction of which the current intensity is several orders higher.
- 2) In forward bias, the initial small voltage is not able to rupture the filaments and the conduction is still ohmic like with no radiative recombination. Therefore, no light emitting is observed in this region. LRS is maintained until the positive voltage is high to repel the mobile defects away from junction area and rupture the filaments (RESET). Although the current abruptly decreases by several orders in HRS, the light-emitting capability restores here, because the radiative recombination instead of filamentary conduction in MQW dominates the current again. By virtue of the defective device property, the forward leakage current mentioned above is realized in the way of trap-assisted diagonal tunneling [25], which will lead to the lower light emission intensity as compared with high-quality LED.

#### IV. CONCLUSION

In summary, the defective InGaN/GaN LED fabricated by MOCVD could simultaneously exhibit light emitting and RS behavior with proper operation. The SET process should be triggered in reverse bias, while the RESET process takes place in forward bias. The RS could be understood as the switching between filament-based ohmic behavior and conventional rectifying behavior in LED. The structural and point defects not only assist the tunneling current in light-emitting HRS (normal LED operation), but also construct the filaments in LRS. The switching voltages in this paper are still quite high, especially the SET voltages, which requires further improvement. However, such bifunctional device could be a potential candidate for futuristic optoelectronic applications.

#### REFERENCES

- [1] A. Bera, H. Peng, J. Lourembam, Y. Shen, X. W. Sun, and T. Wu, "A versatile light-switchable nanorod memory: Wurtzite ZnO on perovskite SrTiO<sub>3</sub>," *Adv. Funct. Mater.*, vol. 23, no. 39, pp. 4977–4984, Oct. 2013.

- [2] C.-W. Chang, W.-C. Tan, M.-L. Lu, T.-C. Pan, Y.-J. Yang, and Y.-F. Chen, "Electrically and optically readable light emitting memories," *Sci. Rep.*, vol. 4, p. 5121, Jun. 2014.
- [3] C. He *et al.*, "Tunable electroluminescence in planar graphene/SiO<sub>2</sub> memristors," *Adv. Mater.*, vol. 25, no. 39, pp. 5593–5598, Oct. 2013.
- [4] M. Ungureanu *et al.*, "A light-controlled resistive switching memory," *Adv. Mater.*, vol. 24, pp. 2496–2500, May 2012.
- [5] N. I. Bochkareva *et al.*, "Defect-related tunneling mechanism of efficiency droop in III-nitride light-emitting diodes," *Appl. Phys. Lett.*, vol. 96, no. 13, p. 133502, Mar. 2010.
- [6] B. Monemar and B. E. Sernelius, "Defect related issues in the 'current roll-off' in InGaN based light emitting diodes," *Appl. Phys. Lett.*, vol. 91, no. 18, p. 181103, Oct. 2007.
- [7] K. Zheng *et al.*, "Resistive switching in a GaO<sub>x</sub>-NiO<sub>x</sub> p-n heterojunction," *Appl. Phys. Lett.*, vol. 101, p. 143110, Oct. 2012.
- [8] Z. G. Ju *et al.*, "Advantages of the blue InGaN/GaN light-emitting diodes with an AlGaIn/GaN/AlGaIn quantum well structured electron blocking layer," *ACS Photon.*, vol. 1, pp. 377–381, Apr. 2014.
- [9] Z.-H. Zhang *et al.*, "On the origin of the electron blocking effect by an n-type AlGaIn electron blocking layer," *Appl. Phys. Lett.*, vol. 104, no. 7, p. 073511, 2014.
- [10] M. S. Ferdous, X. Wang, M. N. Fairchild, and S. D. Hersee, "Effect of threading defects on InGaIn/GaN multiple quantum well light emitting diodes," *Appl. Phys. Lett.*, vol. 91, p. 231107, Dec. 2007.
- [11] X. A. Cao, E. B. Stokes, P. M. Sandvik, S. F. LeBoeuf, J. Kretschmer, and D. Walker, "Diffusion and tunneling currents in GaN/InGaIn multiple quantum well light-emitting diodes," *IEEE Electron Device Lett.*, vol. 23, no. 9, pp. 535–537, Sep. 2002.
- [12] X. A. Cao, J. M. Teetsov, M. P. D'Evelyn, D. W. Merfeld, and C. H. Yan, "Electrical characteristics of InGaIn/GaN light-emitting diodes grown on GaN and sapphire substrates," *Appl. Phys. Lett.*, vol. 85, pp. 7–9, Jul. 2004.
- [13] M. Meneghini, A. Tazzoli, G. Mura, G. Meneghesso, and E. Zanoni, "A review on the physical mechanisms that limit the reliability of GaN-based LEDs," *IEEE Trans. Electron Devices*, vol. 57, no. 1, pp. 108–118, Jan. 2010.
- [14] X. A. Cao, P. M. Sandvik, S. F. LeBoeuf, and S. D. Arthur, "Defect generation in InGaIn/GaN light-emitting diodes under forward and reverse electrical stresses," *Microelectron. Rel.*, vol. 43, pp. 1987–1991, Dec. 2003.
- [15] X. A. Cao, J. A. Teetsov, F. Shahedipour-Sandvik, and S. D. Arthur, "Microstructural origin of leakage current in GaN/InGaIn light-emitting diodes," *J. Crystal Growth*, vol. 264, pp. 172–177, Mar. 2004.
- [16] C. Y. Zhu *et al.*, "Negative capacitance in light-emitting devices," *Solid-State Electron.*, vol. 53, pp. 324–328, Mar. 2009.
- [17] R. X. Wang *et al.*, "Probing deep level centers in GaN epilayers with variable-frequency capacitance-voltage characteristics of Au/GaN Schottky contacts," *Appl. Phys. Lett.*, vol. 89, p. 143505, Oct. 2006.
- [18] A. G. U. Perera, W. Z. Shen, M. Ershov, H. C. Liu, M. Buchanan, and W. J. Schaff, "Negative capacitance of GaAs homojunction far-infrared detectors," *Appl. Phys. Lett.*, vol. 74, pp. 3167–3169, May 1999.
- [19] R. Waser and M. Aono, "Nanoionics-based resistive switching memories," *Nature Mater.*, vol. 6, no. 11, pp. 833–840, Nov. 2007.
- [20] Q. Shan *et al.*, "Transport-mechanism analysis of the reverse leakage current in GaInN light-emitting diodes," *Appl. Phys. Lett.*, vol. 99, p. 253506, Dec. 2011.
- [21] K. Y. Cheong, J. H. Moon, H. J. Kim, W. Bahng, and N.-K. Kim, "Current conduction mechanisms in atomic-layer-deposited HfO<sub>2</sub>/nitrided SiO<sub>2</sub> stacked gate on 4H silicon carbide," *J. Appl. Phys.*, vol. 103, p. 084113, Apr. 2008.
- [22] S. Ganguly, A. Konar, Z. Hu, H. Xing, and D. Jena, "Polarization effects on gate leakage in InAlN/AlN/GaN high-electron-mobility transistors," *Appl. Phys. Lett.*, vol. 101, p. 253519, Dec. 2012.
- [23] S. Yu, X. Guan, and H.-S. P. Wong, "Conduction mechanism of TiN/HfO<sub>x</sub>/Pt resistive switching memory: A trap-assisted-tunneling model," *Appl. Phys. Lett.*, vol. 99, p. 063507, Aug. 2011.
- [24] A. Sawa, "Resistive switching in transition metal oxides," *Mater. Today*, vol. 11, no. 6, pp. 28–36, 2008.
- [25] S. J. Huang *et al.*, "Contrary luminescence behaviors of InGaIn/GaN light emitting diodes caused by carrier tunneling leakage," *J. Appl. Phys.*, vol. 110, p. 064511, Sep. 2011.

Authors' photographs and biographies not available at the time of publication.